



Multipartite entanglement detection based on the generalized state-dependent entropic uncertainty relation for multiple measurements

Li-Hang Ren ^{1,*} Yun-Hao Shi ^{2,3} Jin-Jun Chen,⁴ and Heng Fan^{2,3,5,†}

¹College of Physics and Hebei Key Laboratory of Photophysics Research and Application, Hebei Normal University, Shijiazhuang, Hebei 050024, China

²Institute of Physics, Chinese Academy of Sciences, Beijing 100190, China

³School of Physical Sciences, University of Chinese Academy of Sciences, Beijing 100049, China

⁴School of Science, Tianjin University of Technology, Tianjin 300384, China

⁵Beijing Academy of Quantum Information Sciences, Beijing 100193, China



(Received 13 March 2023; accepted 18 May 2023; published 30 May 2023)

We present the generalized state-dependent entropic uncertainty relations in a multiple measurements setting and the optimal lower bound is obtained by considering different measurement sequences. We then apply this uncertainty relation to witness entanglement and give the experimentally accessible lower bounds on both bipartite and tripartite entanglements. This method of detecting entanglement is applied to a physical system of two particles on a one-dimensional lattice and Greenberger-Horne-Zeilinger (GHZ)-Werner state. It is shown that, for measurements that are not in mutually unbiased bases, this generalized entropic uncertainty relation is superior to the previous state-independent one in entanglement detection. Furthermore, we conduct a demonstration of multipartite entanglement detection of GHZ states up to ten qubits on the QUAUFU cloud quantum computation platform. Our results might play important roles in detecting multipartite entanglement experimentally.

DOI: [10.1103/PhysRevA.107.052617](https://doi.org/10.1103/PhysRevA.107.052617)

I. INTRODUCTION

The uncertainty principle sets limits on the precise prediction of the outcomes of two incompatible measurements, which is originally formulated by variance [1,2]. It is known that entropy is also an uncertainty quantifier, and the entropic uncertainty relation has been constructed in the past decades [3–5]. However, Berta *et al.* found that the uncertainty can be decreased if the measured system is entangled with a quantum memory. Then they proposed a quantum-memory-assisted entropic uncertainty relation [6]. After that, significant progress was made to generalize this entropic uncertainty relation to multiple measurements [7–16].

The lower bounds of these uncertainty relations are known as state independent because the complementary factors come from the overlaps between the eigenstates of measurement operators, which are only connected with measurements. The characteristic of this kind of uncertainty relation is that they are tight for measurements with mutually unbiased bases (MUBs) [17,18]. If the bases of selected measurements are non-MUBs, the inequality is far from tightness. Recently, Bergh and Gärtner proposed a fully state-dependent entropic uncertainty relation, which gave a tighter lower bound for some measurements with non-MUBs [19,20]. However, the generalized state-dependent entropic uncertainty relation for multiple measurements needs to be explored. It remains

interesting whether the generalized uncertainty relation for multiple measurements with non-MUBs is still tighter than the previous one.

The quantum-memory-assisted entropic uncertainty relation has many applications in quantum information, one of which is to witness entanglement [6,19–25]. The detection of entanglement in experiments is important in quantum information processing tasks [26–28]. However, the estimation of entanglement measures requires complete knowledge of the quantum state, which is hard to implement in experiments, especially for high-dimensional states and multipartite states [29]. Thus, lower bounds are usually presented to evaluate entanglement [30–35]. The quantum-memory-assisted entropic uncertainty relation provides an experimentally accessible lower bound on the bipartite entanglement [19,20]. It only needs several measurements and does not rely on the tomography of the quantum state. Therefore, one may ask whether the similar method of obtaining lower bounds on multipartite entanglement can be realized by using the entropic uncertainty relation.

Over the past few years, cloud quantum computation has been available online for various applications, such as tests of fundamental physics [36–42]. Recently, a newly implemented superconducting cloud quantum computation platform was launched online, which is named as SCQ [43]. It was then updated at the QUAUFU cloud quantum computation platform [44]. They successfully generated a ten-qubit Greenberger-Horne-Zeilinger (GHZ) state and verified its fidelity [42]. It is convenient to conduct a demonstration of multipartite entanglement detection on this cloud platform.

*renlihang@hebtu.edu.cn

†hfan@iphy.ac.cn

In this paper, we will prove a generalized state-dependent entropic uncertainty relation for multiple measurements with a pair of referenced measurements. We find that the lower bound of the uncertainty relation depends on the order of measurements, which can be made tighter by taking over all measurement orders. As an application, we apply it to multipartite entanglement detection. On the one hand, this new uncertainty relation provides a lower bound on bipartite entanglement, which is shown in a physical model of two particles governed by the Hubbard Hamiltonian. On the other hand, we give a lower bound on tripartite entanglement by using this new uncertainty relation and the example of the GHZ-Werner state is investigated in detail. Finally, we detect multipartite entanglement of GHZ states from three to ten qubits through the QUAQU cloud quantum computation platform.

II. GENERALIZED STATE-DEPENDENT ENTROPIC UNCERTAINTY RELATIONS FOR MULTIPLE MEASUREMENTS

The quantum-memory-assisted entropic uncertainty relation was first proposed by Berta *et al.* [6], which can be written as

$$S(Q|B) + S(R|B) \geq \log_2 \frac{1}{c} + S(A|B), \quad (1)$$

where $c = \max_{i,j} |\langle q_i | r_j \rangle|^2$ with $\{|q_i\rangle\}$ and $\{|r_j\rangle\}$ being eigenvectors of Q and R , $S(A|B)$ is the conditional von Neumann entropy of state ρ_{AB} , $S(Q|B)$ is the conditional entropy of the postmeasurement state $\rho_{QB} = \sum_i (|q_i\rangle\langle q_i| \otimes I) \rho_{AB} (|q_i\rangle\langle q_i| \otimes I)$, and likewise for $S(R|B)$. If there exist N projective measurements $\{M_m\}_{m=1}^N$ applied on A , the entropic uncertainty relation for multiple measurements is extended to be [7]

$$\sum_{m=1}^N S(M_m|B) \geq -\log_2(b) + (N-1)S(A|B), \quad (2)$$

where

$$b = \max_{i_N} \left\{ \sum_{i_2 \dots i_{N-1}} \max_{i_1} (|\langle u_{i_1}^1 | u_{i_2}^2 \rangle|^2) \prod_{m=2}^{N-1} |\langle u_{i_m}^m | u_{i_{m+1}}^{m+1} \rangle|^2 \right\}, \quad (3)$$

with $|u_{i_m}^m\rangle$ being the i_m th eigenstate of M_m .

Recently, Bergh and Gärtner proposed a fully state-dependent entropic uncertainty relation [19,20], but the generalization for multiple measurements needs to be studied. In the following, we will derive the generalized state-dependent entropic uncertainty relation for multiple measurements, which avoids maximization of the measurement bases' overlaps. Now we consider a set of measurements $\{M_i\}_{i=1}^N$ made on subsystem A and label $|\mathbb{M}_{m_i}^i\rangle$ as the m_i th measurement base of M_i . Denoting measurement X on A and Y on B as a pair of referenced measurements with respective orthonormal bases $\{|\mathbb{X}_x\rangle\}$ and $\{|\mathbb{Y}_y\rangle\}$, the postmeasurement state can be written as

$$\rho_{XY} = \sum_{xy} \Pi_{xy} \rho_{AB} \Pi_{xy}, \quad (4)$$

with $\Pi_{xy} = |\mathbb{X}_x\rangle\langle\mathbb{X}_x| \otimes |\mathbb{Y}_y\rangle\langle\mathbb{Y}_y|$. Before the proof of uncertainty relation, we provide a lemma first.

Lemma 1. Given a pair of referenced measurements (i.e., X on A and Y on B), let M_1, M_2, \dots, M_N be N projective measurements made on A , and the following relation holds:

$$\begin{aligned} & \sum_{i=1}^N S(M_i|B) + H(X|Y) - NS(A|B) - S(\rho_{AB}) \\ & \geq S\left(\rho_{AB} \left\| \sum_{m_N y} \beta_{m_N y}^N \Pi_{m_N y} \right.\right), \end{aligned} \quad (5)$$

where $H(X|Y) = H(XY) - H(Y)$ is the classical conditional entropy with $H(\cdot)$ being the Shannon entropy, the parameter $\beta_{m_N y}^N = \sum_{x m_1 \dots m_{N-1}} c_{x m_1} c_{m_1 m_2} \dots c_{m_{N-1} m_N} p_{x|y}$ with $c_{x m_1} = |\langle \mathbb{X}_x | \mathbb{M}_{m_1}^1 \rangle|^2$ and $c_{m_i m_{i+1}} = |\langle \mathbb{M}_{m_i}^i | \mathbb{M}_{m_{i+1}}^{i+1} \rangle|^2$, and $\Pi_{m_N y} = |\mathbb{M}_{m_N}^N\rangle\langle\mathbb{M}_{m_N}^N| \otimes |\mathbb{Y}_y\rangle\langle\mathbb{Y}_y|$.

This lemma can be proved via an iterative approach [7,45] by applying a set of operations $\{\Lambda_i(\rho) = \sum_{m_i} (|\mathbb{M}_{m_i}^i\rangle\langle\mathbb{M}_{m_i}^i| \otimes I) \rho (|\mathbb{M}_{m_i}^i\rangle\langle\mathbb{M}_{m_i}^i| \otimes I)\}$ on ρ_{XY} , and the proof is shown in Appendix A.

Theorem 1. Given a pair of referenced measurements (i.e., X on A and Y on B), let M_1, M_2, \dots, M_N be N projective measurements made on A and the state-dependent entropic uncertainty relation for multiple measurements reads

$$\sum_{i=1}^N S(M_i|B) + H(X|Y) \geq NS(A|B) + q_1, \quad (6)$$

where $q_1 = -\sum_{m_N y} p_{m_N y} \log_2 \beta_{m_N y}^N$ which is called the complementary factor, the parameter $\beta_{m_N y}^N$ is the same as lemma 1, and $p_{m_N y} = \langle \mathbb{M}_{m_N}^N | \langle \mathbb{Y}_y | \rho_{AB} | \mathbb{M}_{m_N}^N \rangle | \mathbb{Y}_y \rangle$.

Proof. The relation (6) stems from lemma 1 due to the following relation:

$$\begin{aligned} & S\left(\rho_{AB} \left\| \sum_{m_N y} \beta_{m_N y}^N \Pi_{m_N y} \right.\right) \\ & = \text{Tr}(\rho_{AB} \log_2 \rho_{AB}) - \text{Tr}\left(\rho_{AB} \log_2 \sum_{m_N y} \beta_{m_N y}^N \Pi_{m_N y}\right) \\ & = -S(\rho_{AB}) - \sum_{m_N y} p_{m_N y} \log_2 \beta_{m_N y}^N. \end{aligned} \quad (7)$$

We complete the proof of the theorem by substituting Eq. (7) into Eq. (5). ■

The uncertainty relation (6) is derived from the iteration based on the conditional entropy of ρ_{XY} . If we consider the N projective measurements first and apply the operation $\Lambda_{xy}(\rho) = \sum_{xy} \Pi_{xy} \rho \Pi_{xy}$ at last, then the complementary factor will be modified in another way.

Corollary 1. Let M_1, M_2, \dots, M_N be N projective measurements on A . Let X be the referenced measurement on A and Y the referenced measurement on B , then

$$\sum_{i=1}^N S(M_i|B) + H(X|Y) \geq NS(A|B) + q_2, \quad (8)$$

where $q_2 = -\sum_{xy} p_{xy} \log_2 \gamma_{xy}^N$ with the parameter $\gamma_{xy}^N = \sum_{m_1 \dots m_N} (\prod_{i=1}^{N-1} c_{m_i m_{i+1}}) c_{x m_N} p_{m_1 | y}$.

Proof. By iteration with Λ_i at first, an inequality similar to lemma 1 was obtained in Ref. [7]

$$-NS(A|B) + \sum_{i=1}^N S(M_i|B) \geq S(\rho_{AB} \parallel \sigma), \quad (9)$$

where $\sigma = \sum_{m_1 \dots m_N} \prod_{i=1}^{N-1} c_{m_i m_{i+1}} |\mathbb{M}_{m_N}^N\rangle \langle \mathbb{M}_{m_N}^N| \otimes \langle \mathbb{M}_{m_1}^1 | \rho_{AB} | \mathbb{M}_{m_1}^1 \rangle$. Then we apply the operation Λ_{xy} on the right-hand side of Eq. (9) and obtain

$$\begin{aligned} & S(\rho_{AB} \parallel \sigma) \\ & \geq S[\Lambda_{xy}(\rho_{AB}) \parallel \Lambda_{xy}(\sigma)] \\ & = S\left(\rho_{XY} \left\| \sum_{xy} \sum_{m_1 \dots m_N} \prod_{i=1}^{N-1} c_{m_i m_{i+1}} c_{x m_N} p_{m_{1y}} \Pi_{xy} \right.\right) \\ & = -H(\rho_{XY}) - \sum_{xy} p_{xy} \log_2 \sum_{m_1 \dots m_N} \prod_{i=1}^{N-1} c_{m_i m_{i+1}} c_{x m_N} p_{m_{1y}} \\ & = -H(X|Y) - \sum_{xy} p_{xy} \log_2 \gamma_{xy}^N, \end{aligned} \quad (10)$$

where $\gamma_{xy}^N = \sum_{m_1 \dots m_N} \prod_{i=1}^{N-1} c_{m_i m_{i+1}} c_{x m_N} p_{m_{1y}}$ with $p_{m_{1y}} = p_{m_{1y}}/p_y$. Therefore, we complete the proof. ■

It is shown that different measurement orders lead to different complementary factors, which is similar to the results in Ref. [8]. Thus we can obtain the following result by taking the optimal measurement sequence.

Theorem 2. Given the referenced measurement X with a set of measurements $\{M_1, M_2, \dots, M_N\}$ made on A and a referenced measurement Y made on B , let us rearrange the $N + 1$ measurements on A in an order ε . Denoting \mathcal{E}_i as the i th measurement in the ε order with $\{|\mathbb{E}_{\varepsilon_i}^i\rangle \langle \mathbb{E}_{\varepsilon_i}^i|\}$ being its projectors, the optimal entropic uncertainty relation gives

$$\sum_{i=1}^N S(M_i|B) + H(X|Y) \geq NS(A|B) + \max_{\varepsilon} q_{\varepsilon}, \quad (11)$$

where $q_{\varepsilon} = -\sum_{\varepsilon_{N+1}y} p_{\varepsilon_{N+1}y} \log_2 \sum_{\varepsilon_1 \dots \varepsilon_N} p_{\varepsilon_1 y} \prod_{i=1}^N c_{\varepsilon_i \varepsilon_{i+1}}$ is the complementary factor in measurement order ε and the maximization runs over all measurement orders ε .

Proof. Given the order of $N + 1$ measurements $\{X, M_1, M_2, \dots, M_N\}$ made on A , it is easy to obtain an uncertainty relation similar to Theorem 1. Changing the order of measurements, one can obtain $(N + 1)!$ uncertainty relations with different complementary factors. The optimal lower bound is obtained by taking over all measurement orders ε . ■

III. MULTIPARTITE ENTANGLEMENT DETECTION

A. Detecting bipartite entanglement

The entanglement of formation is a useful measure to quantify bipartite entanglement [46,47], which is defined as

$$E_f(\rho_{AB}) = \min_{\{p_i, |\psi_i\rangle\}} \sum_i p_i S(\text{Tr}_B[|\psi_i\rangle \langle \psi_i|]), \quad (12)$$

where the minimum is taken over all ensembles $\{p_i, |\psi_i\rangle\}$ satisfying $\rho_{AB} = \sum_i p_i |\psi_i\rangle \langle \psi_i|$. It's difficult to calculate for

general mixed states. However, it has been known that coherent information $-S(A|B)$ is the lower bound on entanglement of formation [30], which can be used to witness entanglement. From Eq. (11) in Theorem 2, we obtain that

$$-S(A|B) \geq \frac{1}{N} \left[q_m - \sum_{i=1}^N S(M_i|B) - H(X|Y) \right]. \quad (13)$$

Here the parameter q_m refers to the maximal complementary factor by taking over all measurement sequences. To make the terms on the right-hand side measurable experimentally, one needs to apply the data-processing inequality, i.e., $H(M_i|M'_i) \geq S(M_i|B)$ in which $\{M'_i\}_{i=1}^N$ is a set of projective measurements made on B . The lower bound can be obtained experimentally by estimating the complementary factor q_m and classical conditional entropy [namely, $H(X|Y)$ and $H(M_i|M'_i)$], which only needs the probability distribution of measurements. Thus, the entropic uncertainty relation provides a lower bound on coherent information, which can be used to detect entanglement directly.

Next we consider an example of two distinguishable particles on a one-dimensional lattice to estimate the entanglement between two particles. The Hamiltonian is written as

$$H = -J \sum_{p \in \{A,B\}} \sum_{i=1}^{L-1} (\hat{a}_{p,i}^\dagger \hat{a}_{p,i+1} + \text{H.c.}) + U \sum_{i=1}^L \hat{n}_{A,i} \hat{n}_{B,i}, \quad (14)$$

where L lattice sites, J hopping strength, U interaction strength, $\hat{a}_{p,i}^\dagger, (\hat{a}_{p,i})$ the creation (annihilation) operator for particle p and lattice site i , and $\hat{n}_{p,i} = \hat{a}_{p,i}^\dagger \hat{a}_{p,i}$. The Hilbert space of one particle is spanned by the “site basis” $\{|i\rangle\}_{i=1}^L$, which constitute the bases of a natural measurement in this system. The second measurement can be picked as the “tilted basis” measurement, which is realized by letting the system evolve for a period of time and then measuring the particle’s position. The evolution is unitary, which is described as $R(t) = \exp[itH(J = 1, U = 0)]$. We choose the third measurement to be the “tilted basis” measurement with fixed evolution time $t_f = 0.38L$. The preparation of the ground state and the realization of the above measurements were demonstrated in experiments [48–50].

We consider the bipartite entanglement between particles A and B in the ground state of the system with $J = 1$ and $U = -100$. The lower bound of the entanglement of formation can be evaluated by coherent information, which can be detected by Eq. (13). As shown in Fig. 1, the blue solid line and red solid point line correspond to cases of $L = 2$ and $L = 4$ respectively, by using entropic uncertainty relation (11) with three measurements involving site basis $\{|i\rangle\}$, and the tilted basis with evolutions $R(t)$ and $R(t_f)$. Compared with the results that use Eq. (2) to estimate entanglement (blue dot-dashed line for $L = 2$ and red dashed line for $L = 4$), our generalized entropic uncertainty relation is more efficient in detecting entanglement. The blue dotted line is plotted as the detectable entanglement by means of Eq. (11) with the first two measurements in the case of $L = 2$, which is consistent with the results in Refs. [19,20]. Although the increasing number of measurements may reduce the efficiency of entanglement detection, this new uncertainty relation does better for some measurements with non-MUBs. For example, in the case of

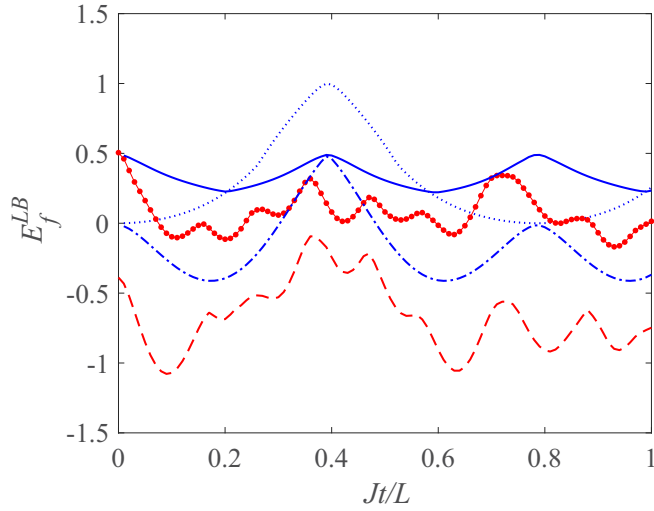


FIG. 1. The lower bound on entanglement of formation E_f^{LB} of the ground state for the system with $J = 1$ and $U = -100$. The blue solid line corresponds to detectable entanglement by using Eq. (11) with three measurements for $L = 2$ while the red solid point line corresponds to the case for $L = 4$. Detectable entanglement are plotted by using Eq. (2) with three measurements for $L = 2$ (blue dot-dashed line) and for $L = 4$ (red dashed line), respectively. The blue dotted line is the case of $L = 2$ by using Eq. (11) with two measurements.

$L = 2$, focusing on the interval of abscissa $[0,0.2]$ and $[0.6,1]$, at which the measurements are not in MUBs, the detectable entanglement with three measurements (blue solid line) is higher than that with two measurements (blue dotted line).

B. Detecting tripartite entanglement

To detect tripartite entanglement, we choose the measure of tripartite entanglement of formation that reads [51]

$$E_F^{(3)}(\rho) = \min_{\{p_i, |\psi_i\rangle\}} \sum_i p_i [S(\rho_A^i) + S(\rho_B^i) + S(\rho_C^i)]/3, \quad (15)$$

where the minimum runs over all the pure state decompositions $\rho = \sum_i p_i |\psi_i\rangle\langle\psi_i|$ and ρ_X^i are the reduced states of subsystem X in state $|\psi_i\rangle$. We choose $1/3$ as the coefficient in Eq. (15) for normalization. The tripartite entanglement of formation is a multipartite entanglement measure that satisfies complete monogamy relation [51]. Consider $\rho_{ABC} = \sum_i q_i |\phi_i\rangle\langle\phi_i|$ as the optimal pure state decomposition and then we have

$$\begin{aligned} E_F^{(3)}(\rho) &= \frac{1}{3} \left(\sum_i q_i S(\rho_A^i) + \sum_i q_i S(\rho_B^i) + \sum_i q_i S(\rho_C^i) \right) \\ &= \frac{1}{3} \left(- \sum_i q_i S(A_i|B_i C_i) - \sum_i q_i S(B_i|A_i C_i) \right. \\ &\quad \left. - \sum_i q_i S(C_i|A_i B_i) \right) \\ &\geq \frac{1}{3} [-S(A|BC) - S(B|AC) - S(C|AB)], \quad (16) \end{aligned}$$

where the second equality uses the relation $S(A_i|B_i C_i) = -S(\rho_A^i)$ for pure state $|\phi_i\rangle$, and the last step is due to the fact that conditional entropy is concave. The above inequality combined with Eq. (13) gives the method to detect tripartite entanglement.

Observation. For a tripartite quantum state ρ_{ABC} , choosing a sets of measurements $\{M_i^A\}$ with referenced measurement X made on subsystem A , and $\{M_i^B\}$ with Y on B , and $\{M_i^C\}$ with Z on C , the tripartite entanglement of formation can be detected by

$$\begin{aligned} E_F^{(3)} \geq & \frac{1}{3N} \left[q_m - \sum_{i=1}^N H(M_i^A|M_i^B M_i^C) - H(X|YZ) \right. \\ & + q'_m - \sum_{i=1}^N H(M_i^B|M_i^A M_i^C) - H(Y|XZ) \\ & \left. + q''_m - \sum_{i=1}^N H(M_i^C|M_i^A M_i^B) - H(Z|XY) \right], \quad (17) \end{aligned}$$

where $H(\cdot|\cdot)$ is the classical conditional entropy, and q_m, q'_m, q''_m are the optimal complementary factors of the corresponding uncertainty relations.

We consider the GHZ-Werner state to estimate the lower bound of $E_F^{(3)}$ via relation (17). The three-qubit state is defined as

$$\rho_p = p|\text{GHZ}\rangle\langle\text{GHZ}| + (1-p)\frac{\mathbf{I}}{8}, \quad (18)$$

where $|\text{GHZ}\rangle = (|000\rangle + |111\rangle)/\sqrt{2}$ is the GHZ state, \mathbf{I} is the identity matrix, and $0 \leq p \leq 1$. Choosing σ_x and σ_z as two measurements made on each qubit, the lower bounds of tripartite entanglement using both Eqs. (2) and (11) are shown in Fig. 2. The results are the same (i.e., the black solid line and red triangles coincide), which indicates that when $p > 0.747614$, tripartite entanglement can be detected in the GHZ-Werner state. However, if we choose measurements σ_z and $\sigma_r = (\sigma_z + \sigma_x)/\sqrt{2}$, which are not in mutually unbiased bases, the entanglement detection efficiency is reduced. In spite of this, the lower bound calculated by means of our relation (11) (red solid point line) is better than the results with the previous uncertainty relation (2) (black dotted line). That is to say, for non-MUBs measurements, the state-dependent uncertainty relation (11) is more effective to detect tripartite entanglement due to the varying overlaps, which is consistent with the results of bipartite entanglement detection [19]. This conclusion holds true for multiple measurements. As shown in Fig. 2, the blue dashed and purple dot-dashed curves correspond to the cases with respective set of measurements $\{\sigma_x, \sigma_y, \sigma_z\}$ and $\{\sigma_x, \sigma_z, \sigma_r\}$ by using Eq. (11). The second is better than the first, and even better than the case with two measurements $\{\sigma_z, \sigma_r\}$ (red solid point line).

Note that a scheme to quantify genuine tripartite entanglement with entropic correlations has been recently proposed [24], where the genuine multipartite entanglement measure

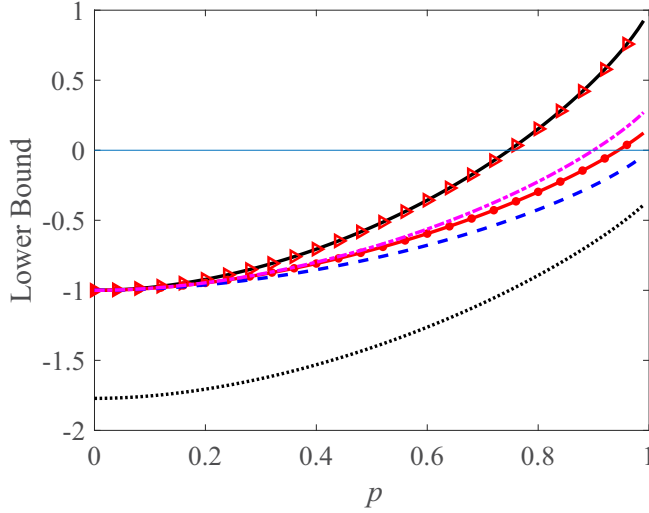


FIG. 2. The lower bound of $E_F^{(3)}$ for GHZ-Werner state. The black solid line and red triangles give the same lower bound by using the uncertainty relations (2) and (11), respectively, with the same set of measurements $\{\sigma_z, \sigma_x\}$. The black dotted line and red solid point line are plotted by using the uncertainty relations (2) and (11), respectively, with two measurements $\{\sigma_z, \sigma_r\}$. The blue dashed and purple dot-dashed curves are obtained by Eq. (11) with a respective set of measurements $\{\sigma_x, \sigma_y, \sigma_z\}$ and $\{\sigma_x, \sigma_z, \sigma_r\}$.

(GMEM) based on entanglement of formation can be estimated by the following inequality [24,52]:

$$E_f^{\text{GME}} \geq -S(A|BC) - S(B|AC) - S(C|AB) - 2 \log_2(d_{\max}), \quad (19)$$

where d_{\max} is the maximal dimension of subsystems A , B , and C . Therefore, if the bases of chosen measurements are non-MUBs, the genuine tripartite entanglement can be detected more effectively by applying this generalized uncertainty relation in a similar way.

C. Generalization in multipartite systems

The procedure of entanglement detection can be extended to a general multipartite systems $\rho_{A_1 \dots A_m}$. The m -partite entanglement measure based on entanglement of formation is defined as [51] $E_F^{(m)} = \min_{\{p_i, |\psi_i\rangle\}} \sum_i p_i E_F^{(m)}(|\psi_i\rangle)$ in which $E_F^{(m)}(|\psi_i\rangle) = \sum_k S(\rho_{A_k}^i)/m$, with $\rho_{A_k}^i$ being reduced state of k -th subsystem A_k for $|\psi_i\rangle$. The lower bound of general m -partite entanglement is derived as follows:

$$E_F^{(m)} \geq \frac{1}{m} \sum_{k=1}^m -S(\rho_{A_k} | \rho_{\bar{A}_k}), \quad (20)$$

where $\rho_{\bar{A}_k}$ is the reduced state after tracing out the subsystem A_k . Here we also choose $1/m$ as the coefficient for normalization. The right-hand side of the above inequality can be estimated by entropic uncertainty relation in a similar way as shown in Eq. (13). Therefore, multipartite entanglement can be detected by means of this method as well.

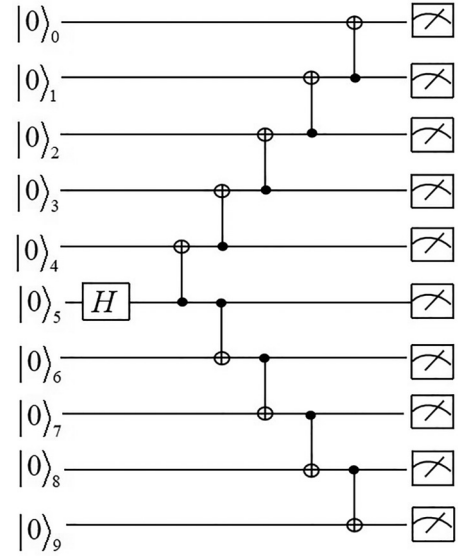


FIG. 3. Quantum circuit of generating a ten-qubit GHZ state.

IV. ENTANGLEMENT DETECTION OF GHZ STATES ON QUAUFU CLOUD QUANTUM COMPUTATION PLATFORM

The present backend devices of the QUAUFU cloud quantum computation platform include one ten-qubit processor (SCQ-P10), one 18-qubit processor (SCQ-P18) and one 50-qubit processor (SCQ-P50). In this demonstration, we take the SCQ-P18 as the backend, which allows single-qubit gates with fidelity $>99\%$ and two-qubit CZ gates with fidelity $95\% - 99.14\%$. The layout and list of device parameters are shown in Appendix B. In this section, we will evaluate multipartite entanglement of GHZ states up to ten qubits. The circuit of preparing the ten-qubit GHZ state is shown in Fig. 3, and the circuits of generating GHZ states from three to nine qubits are designed in a similar way, in which the Hadamard gate acts on the $(n/2)$ th qubit, followed by a series of CNOT gates.

To detect multipartite entanglement $E_F^{(m)}$, we perform two kinds of measurements (namely, σ_z and σ_x), which is the optimal strategy to detect entanglement of GHZ states via the method of entropic uncertainty relations. The results are obtained by averaging 5000 repeated single-shot measurements. The lower bound of $E_F^{(m)}$ can be obtained by Eq. (20) combined with Eq. (13), which only needs the probability distribution of two measurements. The detectable entanglement of n -qubit GHZ states described by the lower bound of $E_F^{(m)}$ are calculated as 0.9980 ± 0.0030 ($n = 3$), 0.9899 ± 0.0148 ($n = 4$), 0.9875 ± 0.0144 ($n = 5$), 0.9868 ± 0.0112 ($n = 6$), 0.8771 ± 0.0386 ($n = 7$), 0.8699 ± 0.0305 ($n = 8$), 0.7347 ± 0.0443 ($n = 9$), and 0.7222 ± 0.0252 ($n = 10$), which are illustrated in Fig. 4. The error bar corresponds to the standard deviation obtained from eight repeated runs. Furthermore, when $n = 3$, the genuine tripartite entanglement can be evaluated by Eq. (19). The lower bound of E_f^{GME} reaches 0.9940 in the three-qubit GHZ state via this method.

We compare the above results with GHZ fidelity. Here the fidelity of GHZ states are defined as $F = (P + C)/2$, where

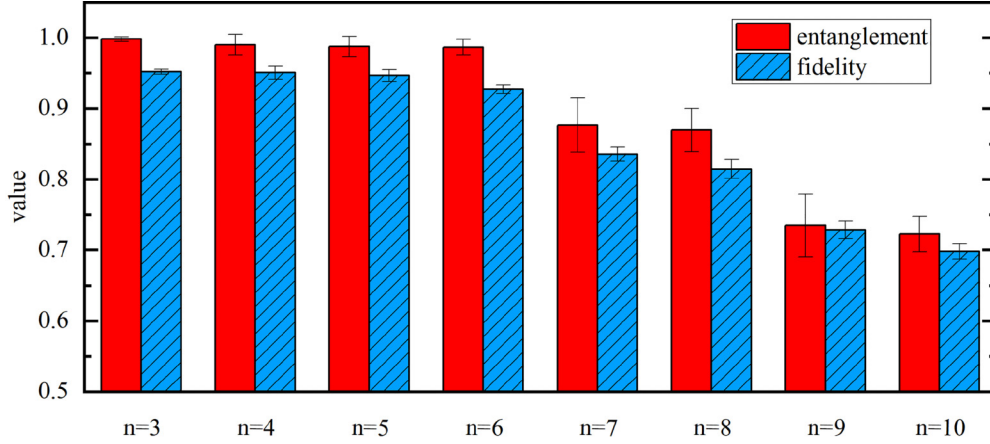


FIG. 4. The lower bound on $E_F^{(m)}$ and fidelity of n -qubit GHZ states. From left to right, the qubits used are $Q_0 - Q_2$, $Q_0 - Q_3$, $Q_0 - Q_4$, $Q_0 - Q_5$, $Q_0 - Q_6$, $Q_0 - Q_7$, $Q_0 - Q_8$, $Q_0 - Q_9$.

P comes from the summation of measurement probabilities $P_{00\dots 0}$ and $P_{11\dots 1}$ and C can be obtained by measuring the parity oscillations [42,53–56]. As shown in Fig. 4, the general multipartite entanglement detected by the entropy uncertainty relation does not differ much from the GHZ fidelity, but the first is slightly higher than the second.

V. DISCUSSION AND CONCLUSION

In conclusion, we propose a generalized entropic uncertainty relation for more than two measurements which is state dependent due to a pair of referenced measurements made on both system and quantum memory. In a multiple measurements setting, the lower bound of the uncertainty relation rely on the sequence of measurements and we give the optimal lower bound by taking over all measurement sequences. We highlight that the quantum-memory-assisted entropic uncertainty relation can be used to detect multipartite entanglement, which requires only the probability distribution of several measurements. By illustrating the examples of the ground state of the Hubbard model and GHZ-Werner state, we show that for measurements with non-MUBs, this generalized uncertainty relation can detect entanglement more efficiently than the previous state-independent one. If the measurements with MUBs are difficult to implement experimentally due to the characteristics of systems or environmental noise, our results are of importance to improve the efficiency of entanglement detection. Finally, we use this method to verify multipartite entanglement of GHZ states up to ten qubits on the QUAUFU cloud quantum computation platform and the detectable entanglement evaluated by means of entropic uncertainty relation only needs the probability distribution of measurements σ_z and σ_x , which can be easily acquired in the experiment.

ACKNOWLEDGMENTS

This work was supported by the NSF-China (Grants No. 12105074 and No. 12004280), Hebei NSF (Grant No. A2019205263), and the fund of Hebei Normal University (Grant No. L2019B07).

APPENDIX A: PROOF OF LEMMA 1

Lemma 1. Given a pair of referenced measurements (i.e., X on A and Y on B), let M_1, M_2, \dots, M_N be N projective measurements on A , and the following relation holds:

$$\begin{aligned} & \sum_{i=1}^N S(M_i|B) + H(X|Y) - NS(A|B) - S(\rho_{AB}) \\ & \geq S\left(\rho_{AB} \left\| \sum_{m_N y} \beta_{m_N y}^N \Pi_{m_N y}\right.\right), \end{aligned} \quad (\text{A1})$$

where $\beta_{m_N y}^N = \sum_{x m_1 \dots m_{N-1}} c_{x m_1} c_{m_1 m_2} \dots c_{m_{N-1} m_N} p_{x|y}$ with $c_{x m_1} = |\langle X_x | M_{m_1}^1 \rangle|^2$ and $c_{m_i m_{i+1}} = |\langle M_{m_i}^i | M_{m_{i+1}}^{i+1} \rangle|^2$, and $\Pi_{m_N y} = |M_{m_N}^N\rangle \langle M_{m_N}^N| \otimes |\Upsilon_y\rangle \langle \Upsilon_y|$.

Proof. This can be proved using an iterative approach [7,45]. First, we prove the relation for $N = 1$. Let M_1 be the measurement on system A with projectors labeled by $\{|M_{m_1}^1\rangle \langle M_{m_1}^1|\}$. Then

$$\begin{aligned} & H(X|Y) - S(A|B) \\ & = H(\rho_{XY}) - H(Y) - S(\rho_{AB}) + S(\rho_B) \\ & = S(\rho_{AB} \parallel \rho_{XY}) - H(Y) + S(\rho_B) \\ & \geq S[\Lambda_1(\rho_{AB}) \parallel \Lambda_1(\rho_{XY})] - H(Y) + S(\rho_B) \\ & = S\left(\rho_{M_1 B} \left\| \sum_{x y m_1} c_{x m_1} p_{x y} \Pi_{m_1 y}\right.\right) - H(Y) + S(\rho_B) \\ & = -S(M_1|B) - \sum_{m_1 y} p_{m_1 y} \log_2 \left(\sum_x c_{x m_1} p_{x y} \right) - H(Y), \end{aligned} \quad (\text{A2})$$

where we denote $H(\cdot|\cdot)$ as the classical conditional entropy, the definition and contractive property of relative entropy are used in the the second the third steps, the measurement operation $\Lambda_1(\rho) = \sum_{m_1} (|M_{m_1}^1\rangle \langle M_{m_1}^1| \otimes I)\rho(|M_{m_1}^1\rangle \langle M_{m_1}^1| \otimes I)$ are used in the fourth step with $c_{x m_1} = |\langle X_x | M_{m_1}^1 \rangle|^2$ and $p_{x y} = \langle X_x | \langle Y_y | \rho_{AB} | X_x \rangle | Y_y \rangle$, and

in the last step $p_{m_1y} = \text{Tr}(\rho_{M_1B} \Pi_{m_1y})$ with $\Pi_{m_1y} = |\mathbb{M}_{m_1}^1\rangle \langle \mathbb{M}_{m_1}^1| \otimes |\mathbb{Y}_y\rangle \langle \mathbb{Y}_y|$. Since $p_{xy} = p_{x|y} p_y$, we have $\log_2(\sum_x c_{xm_1} p_{xy}) = \log_2(\sum_x c_{xm_1} p_{x|y}) + \log_2 p_y$. Then

$$\begin{aligned} & - \sum_{m_1y} p_{m_1y} \log_2 \left(\sum_x c_{xm_1} p_{xy} \right) \\ &= - \sum_{m_1y} p_{m_1y} \log_2 \left(\sum_x c_{xm_1} p_{x|y} \right) - \sum_{m_1y} p_{m_1y} \log_2(p_y) \\ &= - \text{Tr} \left[\rho_{AB} \log_2 \left(\sum_{xym_1} c_{xm_1} p_{x|y} \Pi_{m_1y} \right) \right] \\ & \quad + H(Y) + S(\rho_{AB}) - S(\rho_{AB}) \\ &= S \left(\rho_{AB} \left\| \sum_{xym_1} c_{xm_1} p_{x|y} \Pi_{m_1y} \right. \right) + S(\rho_{AB}) + H(Y). \quad (\text{A3}) \end{aligned}$$

Combining Eqs. (A2) and (A3) gives

$$\begin{aligned} & S(M_1|B) + H(X|Y) - S(A|B) - S(\rho_{AB}) \\ & \geq S \left(\rho_{AB} \left\| \sum_{xym_1} c_{xm_1} p_{x|y} \Pi_{m_1y} \right. \right). \quad (\text{A4}) \end{aligned}$$

By using the contractive property of relative entropy with operation $\Lambda_2(\rho) = \sum_{m_2} (|\mathbb{M}_{m_2}^2\rangle \langle \mathbb{M}_{m_2}^2| \otimes I) \rho (|\mathbb{M}_{m_2}^2\rangle \langle \mathbb{M}_{m_2}^2| \otimes I)$, then

$$\begin{aligned} & S \left(\rho_{AB} \left\| \sum_{xym_1} c_{xm_1} p_{x|y} \Pi_{m_1y} \right. \right) \\ & \geq S \left[\Lambda_2(\rho_{AB}) \left\| \Lambda_2 \left(\sum_{xym_1} c_{xm_1} p_{x|y} \Pi_{m_1y} \right) \right. \right] \\ &= -S(\rho_{M_2B}) + S(\rho_B) - S(\rho_B) + S(\rho_{AB}) - S(\rho_{AB}) \\ & \quad - \text{Tr} \left(\rho_{M_2B} \log_2 \sum_{xym_2} c_{xm_1} c_{m_1m_2} p_{x|y} \Pi_{m_2y} \right) \\ &= S \left(\rho_{AB} \left\| \sum_{xym_2} c_{xm_1} c_{m_1m_2} p_{x|y} \Pi_{m_2y} \right. \right) \\ & \quad - S(M_2|B) + S(A|B), \quad (\text{A5}) \end{aligned}$$

in which $\Pi_{m_2y} = |\mathbb{M}_{m_2}^2\rangle \langle \mathbb{M}_{m_2}^2| \otimes |\mathbb{Y}_y\rangle \langle \mathbb{Y}_y|$. Thus,

$$\begin{aligned} & \sum_{i=1}^2 S(M_i|B) + H(X|Y) - 2S(A|B) - S(\rho_{AB}) \\ & \geq S \left(\rho_{AB} \left\| \sum_{xym_2} c_{xm_1} c_{m_1m_2} p_{x|y} \Pi_{m_2y} \right. \right). \quad (\text{A6}) \end{aligned}$$

By iteration with Λ_i , we can get

$$\begin{aligned} & \sum_{i=1}^N S(M_i|B) + H(X|Y) - NS(A|B) - S(\rho_{AB}) \\ & \geq S \left(\rho_{AB} \left\| \sum_{xym_1 \dots m_N} c_{xm_1} c_{m_1m_2} \dots c_{m_{N-1}m_N} p_{x|y} \Pi_{m_Ny} \right. \right). \end{aligned}$$

Thus we complete the proof. \blacksquare

APPENDIX B: DEVICE PARAMETERS ON QUAUFU CLOUD PLATFORM

In this work, we use SCQ-P18 device on the QUAUFU cloud platform for the demonstrations. The layout of the computing device and its two-qubit gate error rates are shown in Fig. 5. More detailed characteristics of the SCQ-P18 device can be found in Table I.

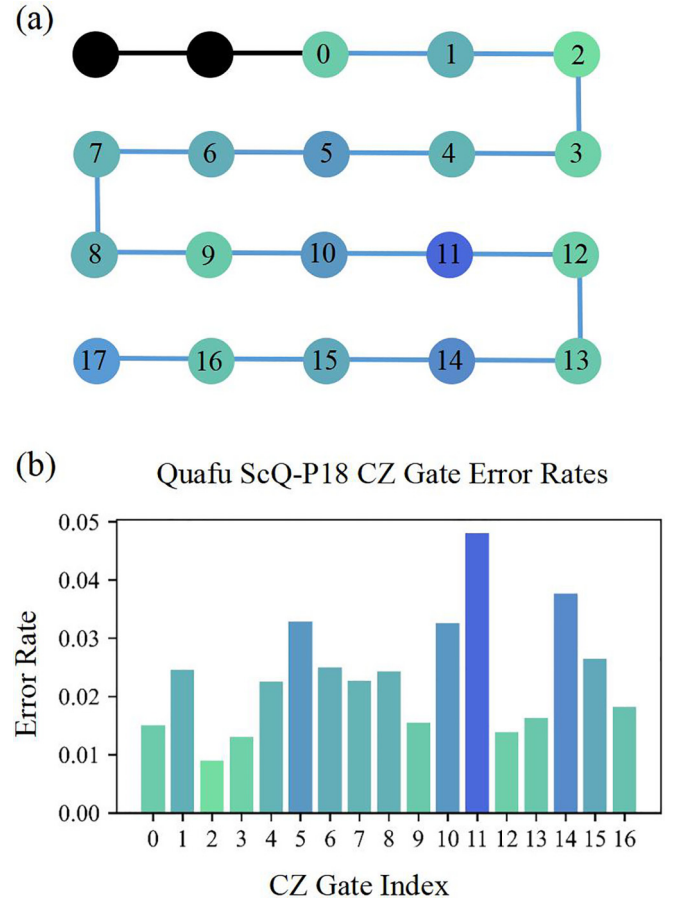


FIG. 5. SCQ-P18 device layout and two-qubit CZ gate error rates. (a) An 18-qubit device layout and connectivity on SCQ-P18. It originally contained 20 qubits and the two qubits marked in black are useless. (b) Error rates for all two-qubit CZ gates on the device.

TABLE I. List of device parameters. The qubit frequency, T1, T2, anharmonicity, readout frequency, and the fidelity of CZ gates are presented.

Qubit index	T1 (μ s)	T2 (μ s)	Qubit frequency (GHz)	Anharmonicity (GHz)	Readout frequency (GHz)	Gate index	CZ Fidelity
0	57.6	4.2	4.590	0.204	6.776	0	0.9850
1	27.9	3.7	5.020	0.192	6.759	1	0.9754
2	41.4	4.8	4.620	0.203	6.737	2	0.9910
3	40.1	2.3	4.977	0.198	6.713	3	0.9870
4	29.0	5.7	4.500	0.205	6.693	4	0.9774
5	36.9	2.1	4.943	0.194	6.676	5	0.9672
6	26.8	3.4	4.566	0.204	6.650	6	0.9750
7	19.8	2.4	5.091	0.200	6.633	7	0.9773
8	23.2	3.5	4.646	0.206	6.625	8	0.9757
9	27.3	1.3	5.038	0.200	6.648	9	0.9845
10	41.2	2.8	4.605	0.205	6.665	10	0.9674
11	28.1	1.5	4.993	0.198	6.693	11	0.9520
12	45.1	3.0	4.545	0.206	6.705	12	0.9862
13	29.8	1.6	4.869	0.198	6.725	13	0.9837
14	45.1	5.5	4.578	0.206	6.751	14	0.9623
15	37.3	3.1	5.048	0.196	6.771	15	0.9735
16	40.8	5.2	4.682	0.203	6.788	16	0.9818
17	41.4	3.1	5.125	0.197	6.807		

- [1] W. Heisenberg, Über den anschaulichen Inhalt der quantentheoretischen Kinematik und Mechanik, *Z. Phys.* **43**, 172 (1927).
- [2] H. P. Robertson, The uncertainty principle, *Phys. Rev.* **34**, 163 (1929).
- [3] D. Deutsch, Uncertainty in Quantum Measurements, *Phys. Rev. Lett.* **50**, 631 (1983).
- [4] K. Kraus, Complementary observables and uncertainty relations, *Phys. Rev. D* **35**, 3070 (1987).
- [5] H. Maassen and J. B. M. Uffink, Generalized Entropic Uncertainty Relations, *Phys. Rev. Lett.* **60**, 1103 (1988).
- [6] M. Berta, M. Christandl, R. Colbeck, J. M. Renes, and R. Renner, The uncertainty principle in the presence of quantum memory, *Nat. Phys.* **6**, 659 (2010).
- [7] S. Liu, L.-Z. Mu, and H. Fan, Entropic uncertainty relations for multiple measurements, *Phys. Rev. A* **91**, 042133 (2015).
- [8] J. Zhang, Y. Zhang, and C.-S. Yu, Entropic uncertainty relation and information exclusion relation for multiple measurements in the presence of quantum memory, *Sci. Rep.* **5**, 11701 (2015).
- [9] Y. Xiao, N. Jing, S.-M. Fei, T. Li, X. Li-Jost, T. Ma, and Z.-X. Wang, Strong entropic uncertainty relations for multiple measurements, *Phys. Rev. A* **93**, 042125 (2016).
- [10] Z. Chen, Z. Ma, Y. Xiao, and S.-M. Fei, Improved quantum entropic uncertainty relations, *Phys. Rev. A* **98**, 042305 (2018).
- [11] S. Wehner and A. Winter, Entropic uncertainty relations – a survey, *New J. Phys.* **12**, 025009 (2010).
- [12] P. J. Coles, M. Berta, M. Tomamichel, and S. Wehner, Entropic uncertainty relations and their applications, *Rev. Mod. Phys.* **89**, 015002 (2017).
- [13] B.-F. Xie, F. Ming, D. Wang, L. Ye, and J.-L. Chen, Optimized entropic uncertainty relations for multiple measurements, *Phys. Rev. A* **104**, 062204 (2021).
- [14] H. Dolatkah, S. Haseli, S. Salimi *et al.*, Tightening the entropic uncertainty relations for multiple measurements and applying it to quantum coherence, *Quantum Inf. Process* **18**, 13 (2019).
- [15] S. Haddadi, M. R. Pourkarimi, and S. Haseli, Multipartite uncertainty relation with quantum memory, *Sci. Rep.* **11**, 13752 (2021).
- [16] H. Dolatkah, S. Haddadi, S. Haseli *et al.*, Tripartite quantum-memory-assisted entropic uncertainty relations for multiple measurements, *Eur. Phys. J. Plus* **137**, 1163 (2022).
- [17] I. D. Ivonovic, Geometrical description of quantal state determination, *J. Phys. A* **14**, 3241 (1981).
- [18] S. Bandyopadhyay, P. O. Boykin, V. Roychowdhury, and F. Vatan, A new proof for the existence of mutually unbiased bases *Algorithmica* **34**, 512 (2002).
- [19] B. Bergh and M. Gärttner, Experimentally Accessible Bounds on Distillable Entanglement from Entropic Uncertainty Relations, *Phys. Rev. Lett.* **126**, 190503 (2021).
- [20] B. Bergh and M. Gärttner, Entanglement detection in quantum many-body systems using entropic uncertainty relations, *Phys. Rev. A* **103**, 052412 (2021).
- [21] C.-F. Li, J.-S. Xu, X.-Y. Xu, K. Li, and G.-C. Guo, Experimental investigation of the entanglement-assisted entropic uncertainty principle, *Nat. Phys.* **7**, 752 (2011).
- [22] R. Prevedel, D. R. Hamel, R. Colbeck, K. Fisher, and K. J. Resch, Experimental investigation of the uncertainty principle in the presence of quantum memory and its application to witnessing entanglement, *Nat. Phys.* **7**, 757 (2011).
- [23] M. Berta, P. J. Coles, and S. Wehner, Entanglement-assisted guessing of complementary measurement outcomes, *Phys. Rev. A* **90**, 062127 (2014).
- [24] J. Schneeloch, C. C. Tison, M. L. Fanto, S. Ray, and P. M. Alsing, Quantifying tripartite entanglement with entropic correlations, *Phys. Rev. Res.* **2**, 043152 (2020).
- [25] X. Zheng, S.-Q. Ma, G.-F. Zhang, H. Fan, W.-M. Liu, and L.-C. Kwek, Multipartite entanglement structure resolution analyzer

- based on quantum-control-assisted multipartite uncertainty relation, *Ann. Phys. (Leipzig)* **533**, 2100014 (2021).
- [26] L. Knips, C. Schwemmer, N. Klein, M. Wieśniak, and H. Weinfurter, Multipartite Entanglement Detection with Minimal Effort, *Phys. Rev. Lett.* **117**, 210504 (2016).
- [27] M. Zwerger, W. Dür, J.-D. Bancal, and P. Sekatski, Device-Independent Detection of Genuine Multipartite Entanglement for All Pure States, *Phys. Rev. Lett.* **122**, 060502 (2019).
- [28] H. Lu *et al.*, Entanglement Structure: Entanglement Partitioning in Multipartite Systems and Its Experimental Detection Using Optimizable Witnesses, *Phys. Rev. X* **8**, 021072 (2018).
- [29] B. Lücke, J. Peise, G. Vitagliano, J. Arlt, L. Santos, G. Tóth, and C. Klempt, Detecting Multiparticle Entanglement of Dicke States, *Phys. Rev. Lett.* **112**, 155304 (2014).
- [30] I. Devetak and A. Winter, Distillation of secret key and entanglement from quantum states, *Proc. Math. Phys. Eng. Sci.* **461**, 207 (2005).
- [31] R. Horodecki, M. Horodecki, and P. Horodecki, Entanglement processing and statistical inference: The jaynes principle can produce fake entanglement, *Phys. Rev. A* **59**, 1799 (1999).
- [32] Z.-H. Chen, Z.-H. Ma, O. Gühne, and S. Severini, Estimating Entanglement Monotones with a Generalization of the Wootters Formula, *Phys. Rev. Lett.* **109**, 200503 (2012).
- [33] Y.-K. Bai, Y.-F. Xu, and Z. D. Wang, General Monogamy Relation for the Entanglement of Formation in Multiqubit Systems, *Phys. Rev. Lett.* **113**, 100503 (2014).
- [34] F. Nicacio and M. C. de Oliveira, Tight bounds for the entanglement of formation of Gaussian states, *Phys. Rev. A* **89**, 012336 (2014).
- [35] Y. Dai, Y. Dong, Z. Xu, W. You, C. Zhang, and O. Gühne, Experimentally Accessible Lower Bounds for Genuine Multipartite Entanglement and Coherence Measures *Phys. Rev. Appl.* **13**, 054022 (2020).
- [36] Y. Chen, M. Farahzad, S. Yoo, and T. C. Wei, Detector tomography on IBM quantum computers and mitigation of an imperfect measurement, *Phys. Rev. A* **100**, 052315 (2019).
- [37] Y. Wang, Y. Li, Z.-Q. Yin, and B. Zeng, 16-qubit IBM universal quantum computer can be fully entangled, *npj Quantum Inf.* **4**, 46 (2018).
- [38] G. J. Mooney, C. D. Hill, and L. C. L. Hollenberg, Entanglement in a 20-qubit superconducting quantum computer, *Sci. Rep.* **9**, 13465 (2019).
- [39] H.-Y. Ku, N. Lambert, F.-J. Chan *et al.*, Experimental test of non-macrorealistic cat states in the cloud, *npj Quantum Inf.* **6**, 98 (2020).
- [40] K. X. Wei, I. Lauer, S. Srinivasan, N. Sundaresan, D. T. McClure, D. Toyli, D. C. McKay, J. M. Gambetta, and S. Sheldon, Verifying multipartite entangled Greenberger-Horne-Zeilinger states via multiple quantum coherences, *Phys. Rev. A* **101**, 032343 (2020).
- [41] Z.-P. Yang, H.-Y. Ku, A. Baishya, Y.-R. Zhang, A. F. Kockum, Y.-N. Chen, F.-L. Li, J.-S. Tsai, and F. Nori, Deterministic one-way logic gates on a cloud quantum computer, *Phys. Rev. A* **105**, 042610 (2022).
- [42] C.-T. Chen, Y.-H. Shi, Z. Xiang, Z.-A. Wang, T.-M. Li, H.-Y. Sun, T.-S. He, X. Song, S. Zhao, D. Zheng, K. Xu, and H. Fan, ScQ cloud quantum computation for generating Greenberger-Horne-Zeilinger states of up to 10 qubits, *Sci. China Phys. Mech. Astron.* **65**, 110362 (2022).
- [43] Code available at <http://q.iphy.ac.cn>.
- [44] Code available at <http://quafu.baqis.ac.cn>.
- [45] P. J. Coles, R. Colbeck, L. Yu, and M. Zwolak, Uncertainty Relations from Simple Entropic Properties, *Phys. Rev. Lett.* **108**, 210405 (2012).
- [46] W. K. Wootters, Entanglement of Formation of an Arbitrary State of Two Qubits, *Phys. Rev. Lett.* **80**, 2245 (1998).
- [47] R. Horodecki, P. Horodecki, M. Horodecki, and K. Horodecki, Quantum entanglement, *Rev. Mod. Phys.* **81**, 865 (2009).
- [48] A. Bergschneider, V. M. Klinkhamer, J. H. Becher, R. Klemt, L. Palm, G. Zürn, S. Jochim, and P. M. Preiss, Experimental characterization of two-particle entanglement through position and momentum correlations, *Nat. Phys.* **15**, 640 (2019).
- [49] M. Boll, T. A. Hilker, G. Salomon, A. Omran, J. Nespolo, L. Pollet, I. Bloch, and C. Gross, Spin- and density-resolved microscopy of antiferromagnetic correlations in fermi-hubbard chains, *Science* **353**, 1257 (2016).
- [50] F. Schäfer, T. Fukuhara, S. Sugawa, Y. Takasu, and Y. Takahashi, Tools for quantum simulation with ultracold atoms in optical lattices, *Nat. Rev. Phys.* **2**, 411 (2020).
- [51] Y. Guo and L. Zhang, Multipartite entanglement measure and complete monogamy relation, *Phys. Rev. A* **101**, 032301 (2020).
- [52] S. Szalay, Multipartite entanglement measures, *Phys. Rev. A* **92**, 042329 (2015).
- [53] T. Monz, P. Schindler, J. T. Barreiro *et al.*, 14-Qubit Entanglement: Creation and Coherence, *Phys. Rev. Lett.* **106**, 130506 (2011).
- [54] C. Song, K. Xu, W. Liu, C. P. Yang, S. B. Zheng, H. Deng, Q. Xie, K. Huang, Q. Guo, L. Zhang *et al.*, 10-Qubit Entanglement and Parallel Logic Operations with a Superconducting Circuit, *Phys. Rev. Lett.* **119**, 180511 (2017).
- [55] C. Song, K. Xu, H. Li *et al.*, Generation of multicomponent atomic Schrödinger cat states of up to 20 qubits, *Science* **365**, 574 (2019).
- [56] A. Omran, H. Levine, A. Keesling *et al.*, Generation and manipulation of Schrödinger cat states in Rydberg atom arrays, *Science* **365**, 570 (2019).